Applied Catalysis B: Environmental 185 (2016) 141–149

Contents lists available at ScienceDirect

Applied Catalysis B: Environmental

journal homepage: www.elsevier.com/locate/apcatb

Selective conversion of sorbitol to glycols and stability of nickel–ruthenium supported on calcium hydroxide catalysts

I. Murillo Leo, M. López Granados, J.L.G. Fierro, R. Mariscal*

Group of Sustainable Energy and Chemistry (EQS), Institute of Catalysis and Petrochemistry (ICP-CSIC), C/Marie Curie 2, Campus de Cantoblanco, 28049 Madrid, Spain

ARTICLE INFO

Article history:
Received 10 September 2015
Received in revised form
28 November 2015
Accepted 2 December 2015
Available online 4 December 2015

Keywords:
Sorbitol
Glycols
Nickel–ruthenium
Alkaline supports
Stability

ABSTRACT

Supported catalysts based on ruthenium have been prepared to study the hydrogenolysis of sorbitol to selectively obtain glycols in an alkaline medium. Among the tested catalysts, ruthenium impregnated directly over $Ca(OH)_2$ exhibited a yield of glycols higher than that of ruthenium supported on an alumina catalyst where the alkali promoter was added separately to the reaction medium. When nickel was incorporated into the calcium hydroxide supported ruthenium catalyst a promoting effect was observed, which was explained by an electronic interaction between both metals. A glycol yield of approximately 40% was accomplished after 4 h of reaction. A number of physicochemical techniques, such as evolved gas analysis by mass spectrometry (EGA-MS), temperature programmed reduction (TPR), X-ray diffraction (XRD), X-ray photoelectron spectroscopy (XPS), and total reflection x-ray fluorescence (TXRF) analysis, were used to characterize fresh and used catalysts. The stability of the NiRuCa catalyst showing the best performance was examined. It was found that it was not stable in the reaction medium because of solubilization of the basic support $Ca(OH)_2$ during the reaction progress. A substantial improvement of the stability was accomplished if the amount of $Ca(OH)_2$ solubilized during the reaction is externally incorporated prior to conducting the reaction.

1. Introduction

Lignocellulosic biomass is presented as an alternative source to replace oil in chemicals production because it is a reservoir of carbon and hydrogen [1]. Cellulose is the major component of lignocellulose (38–50%), and in this field heterogeneous catalysis is gaining increasing interest for transforming cellulose into sugar alcohols such as sorbitol in a single step [2–5]. Sorbitol has been identified as one of the twelve most important building blocks derived from biomass because it has many direct applications or associated reactions that yield other high added-value products [6]. The production of glycols, such as 1,2-propylene glycol (1,2-PG) and ethylene glycol (EG), which are currently used as surfactants, as antifreezing liquids, for the production of polyester resins and for applications in the medical and pharmaceutical industries [7–9], from sorbitol stands out. These glycols are currently derived from oil, therefore production from sorbitol (cellulose) implies a renewable and more environmentally friendly route [10,11].

Sorbitol hydrogenolysis to produce glycols is conducted in the presence of metal catalysts under high H_2 pressure and commonly in the presence of a basic promoter added to the reaction medium. However, metal catalyzed reactions involving polyols present selectivity problems associated with the multitude of possible reactions [12]. The most widely accepted mechanism for this process is based on a first dehydrogenation of sorbitol in the presence of a metal to form an aldose intermediate. The sorbitol hydrogenolysis is promoted by the addition of a basic promoter to the medium, which reduces the energetic barrier to C—C bond cleavage, promoting the retro-aldol condensation required to selectively obtain glycols [8,10,11,13]. Among the solid basic promoters incorporated into the reaction medium, the most commonly used is calcium hydroxide, $Ca(OH)_2$, which is partially insoluble in aqueous media [7,10].

Among the metals used in sorbitol hydrogenolysis to glycols, ruthenium and nickel are by far the most commonly used in previous reports [8,14,15]. High H_2 pressure is required to achieve desirable conversion values when nickel-based catalysts are used.

* Corresponding author. Fax: +34 91 5854760.
E-mail address: r.mariscal@icp.csic.es (R. Mariscal).

http://dx.doi.org/10.1016/j.apcatb.2015.12.005
0926-3373/

Therefore, low ruthenium loading catalysts are widely used in combination with the use of alkaline media. However, the addition of cheaper nickel as a metal promoter is highly recommended due to its excellent C—C bond cleavage ability and it has already been studied in other polyol hydrogenolysis processes [8,10,14,16,17].

Ruthenium supported on SiO_2 catalyst was studied in a pioneering work by Sohounloue et al. [18]. Later, several works studied the catalytic performance of ruthenium supported on activated carbon (AC) or carbon nanotubes and reached glycol yields of 43% at 493 K and 8 MPa of hydrogen pressure after 4 h of reaction [11,19]. More recently, in a study conducted in our laboratory, the catalytic behaviors of Ru catalysts supported on Al_2O_3, SiO_2, TiO_2 and ZrO_2 were studied in the sorbitol hydrogenolysis reaction in the absence of a basic promoter. Ruthenium catalysts supported on alumina have shown the best performance [15]. The use of an oxide with basic character as the support has not been addressed clearly in the case of ruthenium catalysts. In the case of nickel, a study of Ni/MgO catalysts has been reported, and in this case, the leaching of the support in the reaction medium was described [14].

Most work has focused on the catalyst composition, the effect of different reaction parameters on the activity and selectivity and on the determination of the reaction mechanism. However, very few works can be found in the literature that have paid attention to the stability of the catalyst and that have studied the possible causes of deactivation [7,10,13,14,20]. Ye et al. [10] described that a Ce–Ni/Al_2O_3 catalyst prepared via a coprecipitation method showed some improvements in its stability. However, the catalyst was deactivated during sorbitol hydrogenolysis to glycols due to agglomeration of Ni particles during the hydrogenolysis process in the aqueous phase. The recycling test of the Ni_2P/AC catalyst in sorbitol hydrogenolysis showed that the nickel phosphide phase is not stable in aqueous systems, forming a nickel phosphite phase $Ni(PO_3)_2$, and that nickel leached into the liquid reaction mixture [13]. Some encouraging results have been described for the stability of the Ru/C catalyst in hydrogenolysis of xylitol in the presence of a basic promoter in a batch reactor by Sun and Liu [7] and, more recently, in a continuous system with a high-pressure fixed-bed reactor by Auneau et al. [20]. However, an efficient and recyclable solid catalyst for use in alkaline media has not yet been reported for sorbitol hydrogenolysis.

Despite these studies, important points still remain unclear namely the real impact of the alkaline medium, the promoting effects of incorporation of other metals and the catalysts stability. The aim of this work is to study the catalytic activity shown by a ruthenium supported directly on a basic promoter to produce glycols and its comparison with other RuAl (acid support) catalyst under the presence of basic promoters added to the reaction medium. The promoting effect of nickel incorporation was also evidenced, based on the characterization data, a reasonable explanation of the Ni promotion is given. Finally, the stability of the catalyst that showed the best performance was evaluated after reusing the sample five times; adding a base to this catalytic system slows down the deactivation. The physicochemical characterization of fresh and used catalyst will allow identification of the main causes of deactivation.

2. Experimental

2.1. Preparation of catalysts

Two 5 wt.% ruthenium catalysts were prepared via wet impregnation of an aqueous solution of $Ru(NO)(NO_3)_3$ (Alfa Aesar) on γ-Al_2O_3 (surface area of 209 $m^2\,g^{-1}$) and $Ca(OH)_2$ (surface area of ca. 15 $m^2\,g^{-1}$). Both supports were purchased from Sigma–Aldrich. The resulting solids were then dried at 383 K for 12 h. Next, the precursors were subjected to calcination in a 20 vol.% O_2/Ar flow of 100 mL min^{-1} at 623 K (T_{C1}) for 1 h (heating rate of 10 K min^{-1}) and reduction in a 5 vol.% H_2/Ar flow of 100 mL min^{-1} at 473 K (T_{R1}) for 0.5 h (heating rate of 5 K min^{-1}).

With the aim of evaluating the effect of the incorporation of Ni as a promoter, Ni was incorporated on the Ru/$Ca(OH)_2$ precursor via incipient wetness impregnation. In practice, the required amount of $Ni(NO_3)_2{\cdot}6H_2O$ was incorporated to obtain two catalysts with an atomic ratio of Ni/Ru = 1 and 2. After incorporation, the catalysts were dried at 383 K for 12 h. Next, they were treated by calcination under a 20 vol.% O_2/Ar flow of 100 mL min^{-1} at 853 K (T_{C2}) for 1 h (heating rate of 10 K min^{-1}) and reduction in a 5 vol.% H_2/Ar flow of 100 mL min^{-1} at 703 K (T_{R2}) (heating rate of 5 K min^{-1}) for 0.5 h to obtain two catalysts promoted by nickel.

The temperatures of the activation procedures (calcination and reduction) for the samples with and without nickel required to ensure the complete decomposition of ruthenium and nickel precursors and the reduction of the corresponding oxides, were determined using evolved gas analysis by mass spectrometry (EGA-MS, see Fig. S1 in the Supplementary material) and temperature programmed reduction (TPR), respectively (see Fig. 1 below). Table 1 lists the nomenclature, and nominal and experimental composition, the latter determined by TXRF, for the different catalysts prepared in this work.

2.2. Characterization of the catalysts

Evolved gas analysis by mass spectrometry (EGA-MS) was performed by loading the samples in a U-shaped quartz reactor connected to a Balzer Prisma™ quadrupole mass spectrometer (QMS 200). The analysis was conducted while flowing a 20 vol.% O_2/Ar mixture (100 mL min^{-1}) from room temperature to 1000 K at a heating rate of 10 K min^{-1}. The fragments m/z = 17 (H_2O), m/z = 18 (H_2O), m/z = 30 (NO), m/z = 32 (O_2), m/z = 40 (Ar), m/z = 44 (CO_2) and m/z = 46 (NO_2) were continuously monitored using a mass spectrometer. Gas lines from the reactor outlet to the MS inlet were heated at 393 K to avoid H_2O condensation.

Temperature programmed reduction (TPR) experiments were also performed using the U-shaped reactor connected to the mass spectrometer. A 5 vol.% H_2/Ar mixture (100 mL min^{-1}) was flowed while heating from room temperature to 1000 K at a rate of 5 K min^{-1}. In this case, the fragments m/z = 2 (H_2), m/z = 17 (H_2O), m/z = 18 (H_2O) and m/z = 28 (CO) were monitored to evaluate the reduction process.

Powder X-ray diffraction (XRD) patterns were recorded in the 10–90° 2θ range in the scan mode (0.04°, 20 s) using an X'Pert Pro PANalytical diffractometer with Cu K$\alpha_{1,2}$ (l = 0.15418 nm) radiation. The diffractograms were analyzed using the X'Pert HighScore Plus software.

X-ray photoelectron spectra (XPS) were acquired using a VG Escalab 200R spectrometer equipped with a hemispherical electron analyzer and a Mg Kα ($h\nu$ = 1253.6 eV) X-ray source. The activated powder samples were rapidly poured into a flask containing isooctane to prevent oxidation of the samples in the ambient air. Then, the solids were rapidly pressed into a copper holder mounted on a sample rod in the pretreatment chamber of the spectrometer to remove the protecting agent (isooctane). The solids were outgassed at room temperature for 1 h at 10^{-5} mbar to remove isooctane before transfer to the ion pumped analysis chamber. Ru 3d, Al 2p, Ca 2p, Ni 2p, C 1s and O 1s regions were scanned a sufficient number of times to obtain high signal-to-noise ratios. The static charge of the samples was corrected by referencing the binding energies to the metals of the oxide support Al 2p (74.5 eV) and Ca 2p (246.5 eV) levels. The measurement accuracy was ±0.1 eV. The areas of the peaks were computed by fitting the

Table 1
Nomenclature, nominal and experimental composition determined by TXRF analysis of the Ru supported catalysts.

Catalyst[a]	Ru nominal (wt.%)	Ni nominal (wt.%)	Ru content from TXRF (wt.%)	Ni content from TXRF (wt.%)
RuAl-LT	5.0	–	–	–
RuCa-LT and RuCa-HT	5.0	–	5.4	–
NiRuCa-HT	5.0	2.8	5.5	2.7
2NiRuCa-HT	5.0	5.5	5.0	4.8

[a] LT refers to calcination at 623 K and reduction at 473 K and HT refers calcination at 853 K and reduction at 703 K.

experimental spectra to Gaussian/Lorentzian curves after removing the background (using the Shirley function). The surface atom ratios were calculated from the peak area ratios normalized using the corresponding atomic sensitivity factors [21].

Chemical analysis via Total reflection X-ray fluorescence (TXRF) using an Atomika 8030C TXRF spectrometer (Cameca Germany) equipped with a 3 kW Mo/W dual target X-ray tube and a W/C double monochromator multilayer was performed to determine the chemical composition of the solid catalysts and the calcium content in the liquid mixture of products obtained after the reaction. A Si(Li) detector with an active area of 80 mm^2 and a resolution of 150 eV at 5.9 k eV (Mn Kα) was used for the detection and measurement of the produced X-rays.

2.3. Activity measurements

Sorbitol hydrogenolysis reactions were performed in a stainless steel autoclave Parr reactor (100 mL). In a typical experiment, 30 g of aqueous sorbitol solution (20 wt.% sorbitol) and 0.3 g of an activated catalyst (5 wt.% referred to sorbitol) were loaded in the autoclave, which was then flushed several times with N_2 to remove the ambient air. Subsequently, the system was pressurized in H_2 (4 MPa; this pressure was kept constant during the entire experiment), and the mixture was heated to 493 K and stirred at 500 rpm to start the reaction. The reaction was stopped after 4 h. The pH at the beginning and end of the reaction was also measured.

The reaction liquid mixtures were analyzed by HPLC using a Rezex RHM-Monosaccharide H^+ (8%) (300 × 7.80 mm) column and refraction index (RI) and UV (DAD) detectors. The samples for the chromatographic analysis were prepared by adding a known amount of cellobiose as an internal standard. A 0.005 M H_2SO_4 mobile phase was used as the eluent at 313 K with a 0.45 mL min^{-1} flow rate. The sorbitol conversion is defined as the ratio between the number of sorbitol moles consumed in the reaction and the number of sorbitol moles initially present in the mixture. The yield is defined as the ratio of the number of moles of product formed to the total number of moles of sorbitol initially present, taking into account the stoichiometry; the selectivity is defined as the result of dividing the yield value by the sorbitol conversion.

3. Results and discussion

3.1. Catalytic activity of the RuAl catalyst after incorporation of basic hydroxides into the reaction medium

To investigate the effect of adding basic hydroxides to the reaction medium on the catalytic behavior of alumina supported ruthenium, we conducted a series of experiments as shown in Table 2, see entries 1–6. The RuAl-LT catalyst without an alkaline promoter (entry 1) gives 73.9% sorbitol conversion and 19.1% selectivity to glycols, and the yield of glycols is 14.1%. Minor products as C_5 and C_4 polyols (ribitol, xylitol and erythritol), glycerol and others (sorbitan and ethanol) were also detected for this catalyst, but none of them exceeds 7% in selectivity. The pH of the medium changes from 7 to 4 at the end of the reaction, indicating that acid by-products are formed as the reaction progresses. In this case, the carbon balance was comparatively low (53.4%). The formation of some C_1 compounds in the gas phase can be expected based on the formation of C_5 polyols. Ruthenium is the selective species in the sorbitol transformation to glycols because the pure alumina support presents ca. 15% sorbitol conversion, which is entirely selective to polyalcohols with five carbon atoms [15]. Moreover, a blank experiment was conducted with only the basic promoter in the reaction medium (entry 6). In this experiment, 0.9 g of calcium hydroxide was loaded into the reactor under the reaction conditions described in the experimental section, and the sorbitol conversion was negligible, suggesting that a metal catalyst is required to achieve sorbitol transformation selectively to glycols.

Entries 2 and 3 show the results obtained using the RuAl-LT catalyst with two type of basic promoters, KOH and $Ca(OH)_2$, which are completely and partially solubilized, respectively, in the aqueous reaction medium (5 wt.% with respect to loading sorbitol or 0.3 g). The purpose was to examine whether the nature of the alkaline promoter affects the catalytic behavior of RuAl-LT. Both promoters have similar effects, and no significant differences can be observed. The sorbitol conversion decreases to 59.4% and 56.8% for KOH and $Ca(OH)_2$, respectively, whereas the selectivity for glycols is similar to that of the experiment without a basic promotor being therefore the yield to glycols approximately 11%. The presence of a base results in a final pH value of 8, indicating that the base neutralizes the acid by-products formed (the initial pH value of the reaction medium was 14). The carbon balance was improved in both cases, indicating that many of the undetected compounds are not formed at basic pH. The distribution of products is modified due to the disappearance of some compounds, such as erythritol or ethanol, and the appearance of others, such as acetol, but in small amounts.

The effect of the amount of $Ca(OH)_2$ added to the reaction medium was also studied. Entries 1 and 3–5 show the RuAl-LT results after loading 0, 0.3, 0.9 and 1.8 g of $Ca(OH)_2$, equivalent to 0, 5, 15, and 30 wt.% of $Ca(OH)_2$, with respect to sorbitol. By adding more base to the reaction medium, the sorbitol conversion decreases from 73.9% for experiments conducted without $Ca(OH)_2$ to 29.6% when 30 wt.% of basic hydroxide was loaded in the reactor, see entry 5. The product distribution obtained is also clearly modified. In the absence of $Ca(OH)_2$ or when added in small quantities, dehydration products, such acetol, dihydroxyacetone (DHA) or ethanol appear, but all of them vanish with increasing the amount of incorporated base. Moreover, the polyol selectivity increases slightly as the amount of $Ca(OH)_2$ increases, but the main effect is that glycerol and glycols are favored, and the selectivities reached values of 38.1% and 31.7%, respectively, when 1.8 g of $Ca(OH)_2$ was incorporated. However the incorporation of the calcium hydroxide did not improve the glycol yield. It must be also noted that increasing the amount of base added improved the carbon balances, reaching 94.3% in the presence of 30 wt.% $Ca(OH)_2$. Thus, the formation of gas-phase products was minimized because the carbon balance in the absence of the promoter does not exceeded 60%.

In summary, the ruthenium species are those catalytically active and selective and the addition of a basic promoter to the

Table 2
Catalytic activity of the Ru supported catalysts in the hydrogenolysis of sorbitol in basic medium. Reaction conditions: 6 g sorbitol, 24 g H_2O, 0.3 g catalyst, 4.0 MPa H_2, 493 K and 500 rpm stirring speed.

Entry	Catalyst[a]	Basic promoter (g)	X_{Sor} (%)	Products selectivity (%)				$Y_{glycols}$ (%)	C Balance (%)
				Glycols (EG/PG)	Glycerol	Polyols[b]	Others[c]		
1	RuAl-LT		73.9	19.1 (5.5/13.6)	6.5	6.5	6.1	14.1	53.4
2	RuAl-LT	KOH (0.3)	59.4	18.2 (6.3/11.9)	5.6	12.4	6.2	10.8	64.7
3	RuAl-LT	$Ca(OH)_2$ (0.3)	56.8	19.8 (7.4/12.4)	7.2	6.8	5.1	11.2	64.6
4	RuAl-LT	$Ca(OH)_2$ (0.9)	32.5	27.2 (13.2/14.0)	34.8	9.7	0	8.9	90.3
5	RuAl-LT	$Ca(OH)_2$ (1.8)	29.6	31.7 (16.3/15.4)	38.1	13.0	0	9.4	94.3
6		$Ca(OH)_2$ (0.9)	4.0	0	0	0	0	0	96.0
7	RuCa-LT		82.1	27.8 (11.8/16.0)	7.7	4.4	18.2	22.8	65.0
8	RuCa-LT	$Ca(OH)_2$ (1.8)	74.2	35.0 (16.7/18.3)	51.3	9.4	0	25.9	95.6
9	RuCa-HT		84.1	33.6 (10.2/23.4)	7.6	6.4	14.1	28.3	66.8
10	NiRuCa-HT		89.2	44.6 (14.7/29.9)	4.2	4.7	21.3	39.7	76.8
11	2NiRuCa-HT		80.5	50.1 (16.2/33.9)	4.8	3.7	20.0	40.3	82.2
12	NiRuCa-HT	$Ca(OH)_2$ (0.3)	93.6	49.5 (15.5/34.0)	11.5	4.2	17.2	46.3	82.8

[a] LT refers to calcination at 623 K and reduction at 473 K and HT refers to calcination at 853 K and reduction at 703 K.
[b] Polyols: ribitol, xylitol and erythritol.
[c] Others: sorbitan, acetol, ethanol and dihydroxyacetone.

reaction medium does not improve the yield of glycols because the increasing selectivity to glycols was countered by the decreasing sorbitol conversion. For experiments with the highest precursor amount (0.9 and 1.8 g of $Ca(OH)_2$), an increase in conversion to polyols and, in particular, glycerol was observed. The use of basic additives in the reaction medium is also very positive in terms of carbon balance. This implies that unreacted sorbitol can now be recycled and reintroduced as a reagent into the reactor for a new reaction.

3.2. Ruthenium catalysts supported on basic calcium hydroxide

Taking into account the positive effect of the presence of $Ca(OH)_2$ in the reaction medium for selectivity to glycols and glycerol, it was decided to support Ru particles directly on calcium hydroxide. The results obtained from the RuCa-LT catalyst are shown in entry 7 of Table 2. This catalyst presents better performance than the catalyst prepared using Al_2O_3 as support (entry 1). Sorbitol conversion reached a value of 82.1% with a selectivity for glycols of 27.8%, which implies a glycol yield of 22.8%. Carbon balance (53.4%) is also better than that of alumina catalyst. Next, the same experiment was conducted with incorporation of calcium hydroxide into the aqueous solution (entry 8). A trend similar to the RuAl-LT catalyst was observed. The incorporation of a base in the reaction medium results in a slight decrease of sorbitol conversion (74.2%) along with a slight increase in the glycol selectivity (35.0%) and yield to (25.9%). Moreover, when compared with the results of entry 7, there was a significant increase in the selectivity to glycerol (51.3%) and an improvement of the carbon balance because the only reaction products detected were polyols C_5, glycerol and glycols. However when the results of entry 8 (RuCa-LT) are compared with those of entry 5 (alumina supported catalyst), the conversion of sorbitol increases significantly from 29.6 to 74.2%, the selectivity to glycols is slightly higher (35.0 versus 31.7%), and so does the glycol yield from 9.4% to 25.9%. In addition, the selectivity to glycerol is higher with ruthenium supported on calcium hydroxide (51.3%). For both catalysts, the carbon balance is approximately 95%.

The good activity exhibited by this catalyst could be due in part to the role of ruthenium, which favors dehydrogenation/hydrogenation reactions, and the amount of base used as a support anchored in the catalyst, resulting in C—C bond cleavage by the retro-aldol condensation mechanism. In general, it seems that a basic pH (the presence of OH^-) has the same role for both acidic or basic supports because it causes the sorbitol conversion to decrease, the carbon balances to improve and the glycerol yield to increase significantly, making it the main product obtained under our reaction conditions. To conclude, the best results were reached when ruthenium was directly impregnated on $Ca(OH)_2$ indicating that a closer contact between the metal and the support is more beneficial in terms of conversion, yield of glycols and carbon balance that adding $Ca(OH)_2$ to the reaction medium.

3.3. Promotion of catalytic activity by Ni incorporation on the RuCa-HT catalyst

With the goal of further improving the catalytic performance of these catalysts and to increase the yield of glycols, the effect of adding a metal promoter to RuCa-HT was studied. Nickel was selected because, as stated in the literature, it shows a high hydrogenation capacity [10,16]. Nickel promoted catalysts were prepared with a Ni/Ru atomic ratio of 1(NiRuCa-HT) and 2 (2NiRuCa-HT). Catalysts promoted with nickel, as shown later, required to be activated at higher temperatures of calcination and reduction, 853 K and 623 K respectively. Consequently, for comparison purposes the RuCa precursor must be activated at the same temperatures than those used for bimetallic NiRu catalysts. The catalytic properties of RuCa-HT were summarized in the entry 9. The most relevant result for the RuCa-HT catalyst when compared to RuCa-LT (entry 7), was a slight improvement in the selectivities for glycols, which improved from 27.8% to a 33.6%. Moreover, the EG/PG ratio decreased in the RuCa-HT catalyst, indicating more selectivity to propylene glycol.

The NiRuCa-HT catalyst (entry 10) shows some differences when compared to RuCa-HT catalyst: a slight increase in sorbitol conversion, glycol selectivity and yield and carbon balance. In other words the presence of Ni favors the production of glycols (yield of 39.7%). For the 2NiRuCa-HT catalyst (entry 11), the glycol yield practically did not improve due to the decrease in sorbitol conversion; however, the selectivity to glycols increased. Based on these results, in the presence of more nickel, the sorbitol conversion decreases with respect to the other products and reaches 80.5% after 4 h. The selectivity for the products of interest increases to 50.1% with 2NiRu/$Ca(OH)_2$, but the yield of 1,2-PG and EG increased slightly compared with NiRuCa-HT, reaching almost the same value (40.3%) after 4 h. of reaction. The product distribution is similar to that with the other catalyst, but the carbon balance improves, reaching 82.2% at the end of the reaction. Finally, the NiRuCa-HT catalyst was also tested in the presence of the basic promoter $Ca(OH)_2$ (entry 12), where the sorbitol and glycol conversions increased and achieved a glycol yield of 46.3%. In summary, the

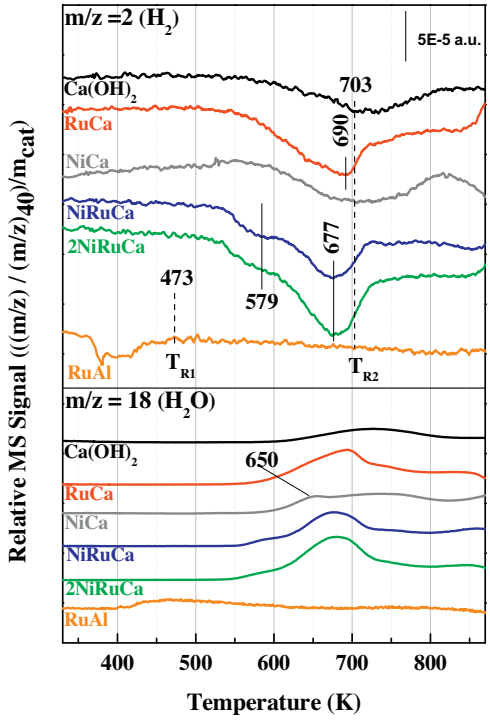

Fig. 1. H_2-TPR profiles obtained during H_2/Ar treatment of the Ru calcined samples.

promoter effect of nickel in this type of catalyst was clear, where an atomic ratio of Ni/Ru = 1 is sufficient to reach a glycol yield of 46.3%.

3.4. Characterization of the Ru and NiRu catalysts

The reducibility of the calcined catalysts was studied using H_2-TPR. The profiles of the different catalysts are displayed in Fig. 1, where the signals $m/z = 2$ (H_2 consumption) and $m/z = 18$ (removed H_2O) are represented. The Ru/Al_2O_3 sample was calcined at 623 K for 1 h with 100 mL min^{-1} of 20 v/v% O_2/Ar flow before the H_2-TPR experiment. This sample has a hydrogen consumption peak in the range of 350–450 K, which is attributed to the reduction of $Ru^{\delta+}$ species in RuO_x to metallic ruthenium (Ru°) [22,23]. Ruthenium supported on $Ca(OH)_2$ samples was calcined at 853 K (Tc_2) for 1 h with 100 mL min^{-1} of 20 v/v% O_2/Ar flow before the H_2-TPR experiments. $Ca(OH)_2$ shows a small and broad peak for H_2 and H_2O patterns at high temperatures in the range 650–800 K, which could be associated with surface impurities on this support. In contrast, the RuCa calcined sample presents a hydrogen consumption peak with a maximum centered at 690 K. Compared with Ru/Al_2O_3, the interaction of ruthenium with this second support is much stronger because its reduction occurs at significantly higher temperatures. A reference sample (labeled as NiCa) with nickel (5 wt.%) supported on calcium hydroxide was also analyzed. Sample was also calcined at 853 K for 1 h before TPR. Regarding the hydrogen profile, this is very similar to that of $Ca(OH)_2$ although the H_2 consumption is somewhat higher. For $m/z = 18$ profile (evolution of H_2O), an extra peak is observed at around 650 K that is associated to the reduction of nickel oxide to metallic nickel. When nickel is incorporated to the RuCa precursor (NiRuCa and 2NiRuCa samples), the hydrogen consumption peak maxima shifted to lower temperatures (677 K), clearly suggesting that the presence of nickel facilitates the reduction of ruthenium possibly due to an interaction between both elements. In contrast, a shoulder is also observed at 579 K, which can be attributed to the reduction of the nickel oxide to metallic nickel. This lower temperature compared to the monometallic NiCa sample could be due to a smaller particle size for nickel oxide in bimetallic samples. In summary, we can say that the reduction profiles of these samples indicate that the interaction of Ru with the basic $Ca(OH)_2$ support is stronger than that with alumina. Furthermore, a certain interaction between the nickel and ruthenium appears to exist because it facilitates ruthenium reducibility.

According to the H_2-TPR results, the reduction temperature at 703 K for 0.5 h with 100 mL min^{-1} of 5 v/v% H_2/Ar transforms the metal oxides into metallic species. To prevent sintering of the ruthenium and nickel, a reduction temperature only slightly higher than that of the maximum of the TPR H_2 consumption peaks was selected.

XRD patterns of the ruthenium catalysts studied in this work are shown in Fig. 2. The RuAl-LT diffractogram (see Fig. 2A) shows peaks corresponding to γ-Al_2O_3 with a tetragonal structure (1, JCPDS 00-046-1131), and to Ru° (2, JCPDS 00-006-0663) was observed for a reflection at $2\theta = 38.7$, 44, 58.5, 78.5 and a shoulder at 86°, which overlaps with some of the most important diffraction peaks of Al_2O_3. For catalysts supported on $Ca(OH)_2$ (see Fig. 2B), the peak of the Ru° phase is not observed, suggesting that the ruthenium in this sample has a small particle size and a high dispersion on this support. The diffraction peaks associated with metallic Ni, RuO_x, NiO or solid solutions of Ru–Ni phases are not observed in the rest of the catalysts. Therefore, the peaks appearing in each diffractogram make reference to the phases of the support. RuCa-LT presents peaks of $Ca(OH)_2$ with a hexagonal structure (3, JCPDS 01-081-2040) with lower intensity than for the same support in the absence of ruthenium. The diffraction peaks associated with metallic ruthenium are not observed, which suggests that ruthenium has good dispersion on this support compared with alumina. The same catalyst activated at a higher temperature, RuCa-HT, showed diffraction peaks attributed to $Ca(OH)_2$ (3) and peaks corresponding to calcium oxide (4). Since this sample has been calcined at higher temperature, Ca hydroxide has been dehydrated to CaO. The catalysts containing nickel as a metallic promoter (NiRuCa-HT and 2NiRuCa-HT) show diffraction peaks associated with calcium oxide with a cubic structure (4, JCPDS 00-037-1497). The phases of the support present in activated catalysts depend mainly on the thermal effect of the activation process (see Fig. S2 in Supplementary material), although the presence of the ruthenium precursor slightly inhibits the dehydration of the calcium hydroxide to calcium oxide during the activation. In summary, ruthenium and nickel show no diffraction peaks when supported on calcium hydroxide independently they are activated at high or low temperatures, indicating good dispersion of both metals in these samples.

X-ray photoelectron spectra (Ru 3d and Ni 2p regions, Fig. 3) of the RuAl-LT, RuCa-LT, RuCa-HT, NiRuCa-HT and 2NiRuCa-HT catalysts were measured with the aim of identifying the oxidation state of the ruthenium and nickel species present on the catalyst surface and the relative surface atomic ratio for the different metals. The peak corresponding to Ru $3d_{3/2}$ is overlapping with the C 1s peak and less attention was given to. Therefore, the carbon peak is not used as the reference, and the metal of the oxide or hydroxide used as the support in each catalyst was taken as the reference: Al 2p (74.5 eV) for RuAl-LT [22] and Ca 2p (346.5 eV) for metals supported on $Ca(OH)_2$ catalysts [24].

Fig. 3A shows the XPS spectra of the Ru 3d region for the different ruthenium supported catalysts. The ruthenium species in this region present a doublet associated with the $3d_{5/2}$ and $3d_{3/2}$ levels; the latter is half as intense as the former peak and is placed at a binding energy of 4.1 eV higher than $3d_{5/2}$. This region is more complex because there is also a peak associated with the C 1s (284.6 eV) level due to adventitious hydrocarbons and another peak centered at approximately 289–290 eV corresponding to

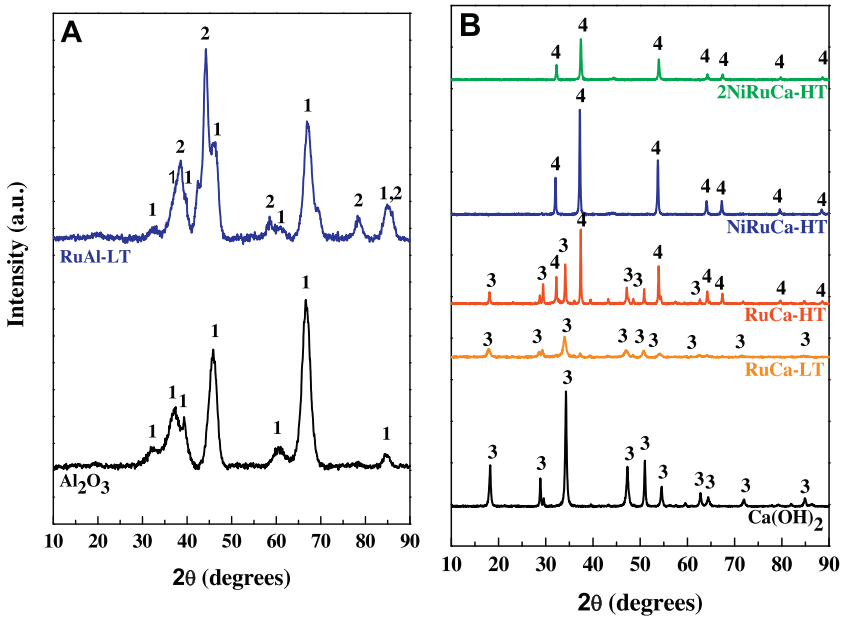

Fig. 2. X-ray diffraction patterns of the Ru-supported catalysts; (1) Al_2O_3 (JCPDS 00-46-1131), (2) Ru° (JCPDS 00-06-0663), (3) $Ca(OH)_2$ (JCPDS 01-081-2040) and (4) CaO (JCPDS 00-37-1497).

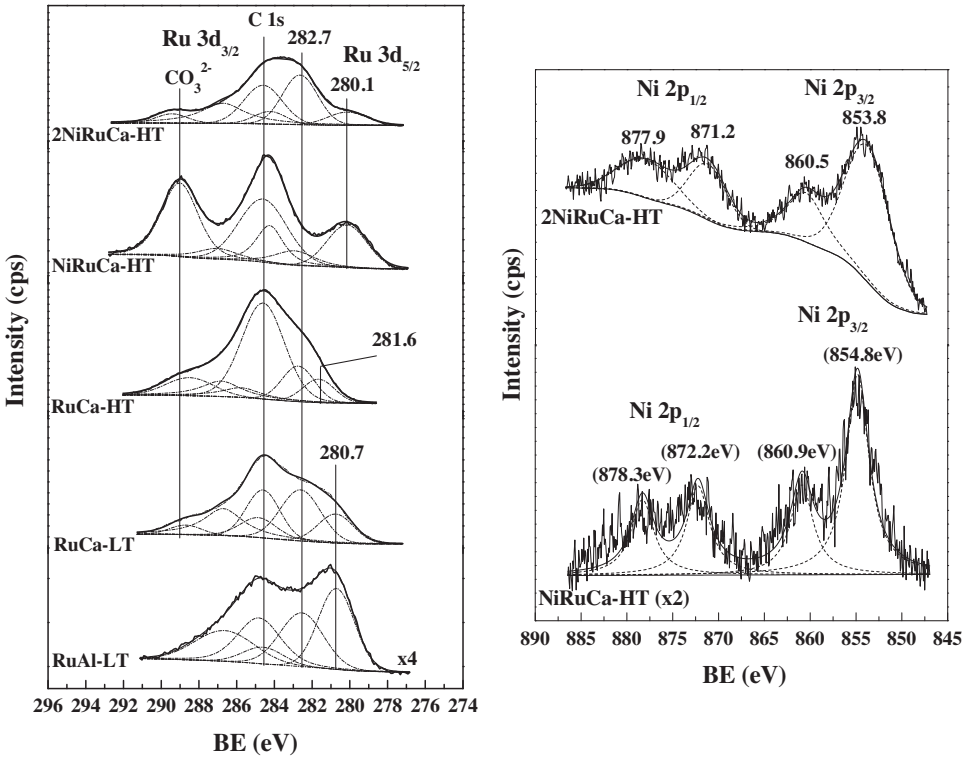

Fig. 3. Ru 3d and Ni 2p XPS spectra obtained for the Ru activated catalysts.

the C 1s level and attributed to the CO_3^{2-} [24] present in the catalysts supported on $Ca(OH)_2$ (RuCa-LT, RuCa-HT, NiRuCa-HT and 2NiRuCa-HT). We will pay attention to the spectral region between 278 and 284 eV, which corresponds to Ru $3d_{5/2}$ core level. This region shows two contributions which are attributed to Ru° and partially oxidized ruthenium ($Ru^{\delta+}$) species [22,25–27]. The first contribution is centered at 280.1 eV for catalysts containing nickel (NiRuCa-HT and 2NiRuCa-HT), at 280.7 eV for RuAl-LT and RuCa-LT catalysts and at 281.6 eV for RuCa-HT samples. Those peaks were attributed to ruthenium in a completely reduced state (Ru°), the shift to higher binding energies shown by RuCa-HT catalysts indicates that, despite the activation procedure, ruthenium is slightly more oxidized than the rest of the samples, which might suggest a greater interaction between ruthenium and support. In addition, in all the catalysts, a second contribution is found at approximately 282.7 eV, which is related to partially oxidized ruthenium species ($Ru^{\delta+}$) [22,26].

Fig. 3B displays the Ni 2p level for the NiRuCa-HT and 2NiRuCa-HT catalysts. In both Ni $2p_{3/2}$ spectra, nickel satellite peaks appear at 860 eV, which is caused by the loss of kinetic energy of the photoelectron emitted to excite a valence electron to an unoccupied orbital, along with a peak at 854.8 eV for NiRuCa-HT and at 853.8 eV for the 2NiRuCa-HT level. According to the literature, binding energies of 854–855 eV correspond to Ni^{2+} species [28]. In our case, there is a shift to lower binding energies of 854.0 eV in 2NiRuCa-HT. Therefore, Ni° and Ni^{2+} species coexist on 2NiRuCa-HT catalysts, and Ni^{2+} is the primary species present on the NiRuCa-HT surface; the presence of nickel in the oxidized state is confirmed by the presence of the satellite peak, which is characteristic of this type of nickel. Therefore, these results suggest that there is an electronic transfer from Ni to Ru, which is much clearer for the NiRuCa-HT catalyst. If the Ni proportion increases, the proportion of Ni atoms with no interaction with Ru atoms increases and the shift is less evident. The promoting effect of nickel and this electronic transfer between nickel and ruthenium can be associated.

Table 3 summarizes the binding energies reported for ruthenium and nickel in all the catalysts tested. In this table, the surface atomic ratios of Ru/Ca, Ni/Ca and Ni/Ru are also given. Based on these results, the RuCa-LT catalyst has more ruthenium exposed on the surface. However, 67% of the total ruthenium is partially oxidized, whereas on RuCa-HT, 61% is oxidized, representing the majority of ruthenium species. The RuAl-LT catalyst has almost half of its ruthenium reduced, and the other half is $Ru^{\delta+}$ species (Ru/Al = 0.15). Of the catalysts that incorporate nickel, NiRuCa-HT has the highest proportion of reduced ruthenium species on its surface (70%), which is possibly the cause for its better activity in sorbitol hydrogenolysis. In the 2NiRuCa-HT catalyst, most of the exposed nickel appears as Ni^{2+} species, so no complete reduction of nickel species is achieved during the activation procedure. The Ru/Ca atomic ratio is lower than in the monometallic catalysts. The Ni/Ru atomic ratio is lower than the theoretical atomic relationships in both of them, and the Ni/Ru ratio was similar in both catalysts and was below the expected ratio based on the catalyst preparation, although 2NiRuCa-HT was impregnated with more nickel. In summary, based on the XPS data, a large amount of the surface exposed ruthenium must be present in the metallic state. The promoter effect of nickel is precisely that there is a charge transfer from nickel to ruthenium. If the nickel load is increased, this charge transfer is not as effective.

The discussion of the catalytic behavior and characterization data regarding the physicochemical properties can be summarized as follows: the glycol yield of the RuAl-LT catalyst was not improved by performing the hydrogenolysis of sorbitol in an alkaline medium. However, a clear decrease in the conversion of sorbitol associated with increased selectivity to glycols is observed. In contrast, when ruthenium is supported directly on the basic promoter $Ca(OH)_2$, a noticeable increase in the glycol yield was observed, suggesting that the intimate contact between the ruthenium metal and the basic promoter is important, which is confirmed by the strong interaction of Ru with the $Ca(OH)_2$ support (based on the TPR profiles) and high dispersion (no XRD diffraction peaks are observed). The promoting effect of nickel on the Ru/$Ca(OH)_2$ catalyst is clear after observing the activity measurement. This result is associated with the reducibility of Ru (the maximum is at a lower temperature, see the TPR results) possibly due to some metal–metal interactions. The interaction between nickel and ruthenium is confirmed by XPS data, where a charge transfer from nickel to ruthenium is clearly observed, at least for the NiRuCa-HT catalyst. Therefore, it is considering the most widely accepted mechanism for this reaction [8,10,11,13] this interaction between metallic species of Ni and Ru in the presence of the basic promoter should promote dehydrogenation from sorbitol to form some intermediates, which are hydrogenated to form the products of interest.

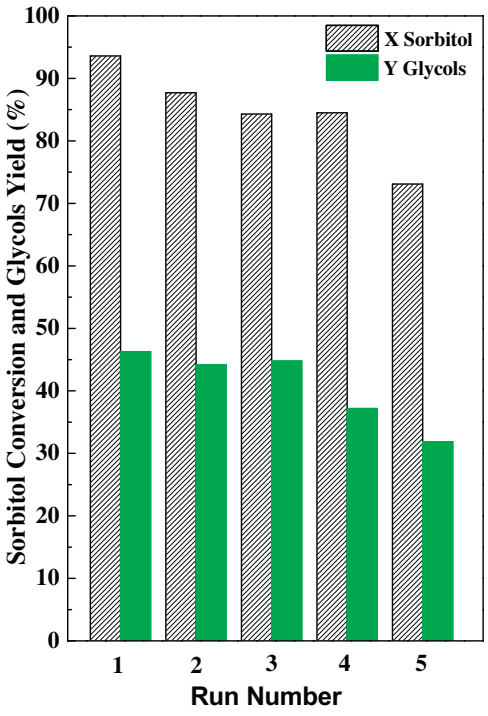

Fig. 4. Reutilization test for the NiRuCa-HT catalyst.

3.5. *Reusability of the NiRuCa-HT catalyst and its characterization after reaction*

The NiRuCa-HT catalyst, that with the most promising catalytic behavior, was reused for five times. The solid catalyst was separated from the reaction liquid and then it was dried in an oven at 383 K for 12 h. Once dried and weighed, a loss of catalyst about 85 wt.% was observed, only 15 wt.% of the catalyst (47.9 mg) was recovered after its use in reaction. Based on this fact, the catalyst was not stable in the reaction medium due to high solubility of the $Ca(OH)_2$ support during the reaction. Consequently, and with the aim of reusing this catalyst in more than one reaction cycle, it was decided to incorporate the same amount of $Ca(OH)_2$ lost in the first run as a sacrificial agent to prevent greater loss of the support and allow for reuse of the NiRuCa-HT catalyst. After the second run and the separation of the solid catalyst from the reaction products via centrifugation, the catalyst was reloaded into the reactor along with a fresh sorbitol solution and 0.275 g of $Ca(OH)_2$ for a new reaction cycle. The results are shown in Fig. 4. The NiRuCa-HT catalyst showed a stable yield of glycols for three runs and decreases moderately in the fourth and fifth runs. At this point, it is necessary to emphasize that the amount of $Ca(OH)_2$ loaded in each run is relatively low (4.6 wt.% with respect to sorbitol) in comparison to other works, where the basic promoter incorporated reached 15 wt.% of sorbitol [11]. The glycol yield changes from 46.3% (run 1) to 32.0% (run 5). During this procedure, the $Ca(OH)_2$ acts as a sacrificial agent to ensures that the reaction remains under alkaline conditions. To determine the amount of $Ca(OH)_2$ to replenish after each cycle, chemical analysis of the liquid reaction products using total reflection X-ray fluorescence (TXRF) analysis to quantify the amount of Ca leaching is required. The calcium content was exactly 275.2 mg of the $Ca(OH)_2$ solubilized in the reaction liquid. It should be noted that ruthenium and nickel was not detected by TXRF in the liquid after reaction, therefore leaching of the active metals in

Table 3
Binding energies of the Ru 3d and Ni 2p levels, and Ru/X, Ni/X and Ni/Ru atomic ratios for the different catalysts.

Catalyst	BE_{Ref} (eV)	Ru $3d_{5/2}$ (eV)	Ni $2p_{3/2}$ (eV)	Ru/Ca	Ni/Ca	Ni/Ru
RuAl-LT	Al 2p (74.5) Al_2O_3	280.7 (55) 282.5 (45)	–	–	–	–
RuCa-LT	Ca 2p (346.5) $Ca(OH)_2$	280.8 (33) 282.6 (67)	–	0.28	–	–
RuCa-HT		281.6 (39) 282.7 (61)	–	0.17	–	–
NiRuCa-HT		280.0 (70) 281.5 (30)	854.8	0.07	0.03	0.38
2NiRuCa-HT		280.1 (22) 282.6 (78)	853.8	0.12	0.05	0.44
NiRuCa-HT used 1 run	Ca 2p (347.6) $CaCO_3$	280.2 (54) 282.1 (46)	852.3 855.8 857.5	0.83	0.80	0.97
NiRuCa-HT used 5 runs		280.1 (62) 282.2 (38)	852.3 855.1 857.3	3.29	5.58	1.7

The values of the proportional areas of the Ru° and $Ru^{\delta+}$ species are shown in brackets.

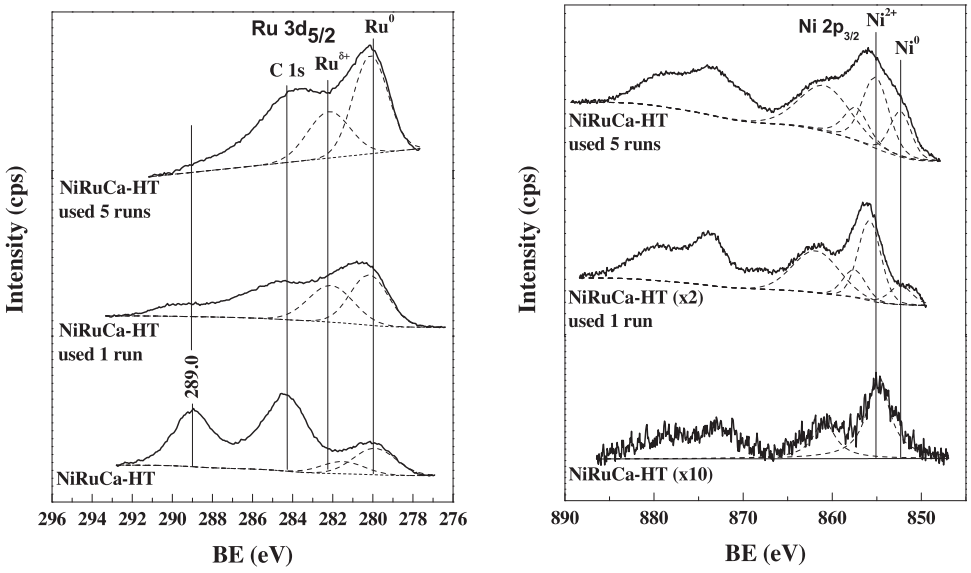

Fig. 5. Ru 3d and Ni 2p XPS spectra of the used NiRuCa-HT catalyst after different runs.

the reaction medium does not occur. Thus, the NiRuCa-HT catalyst shows good catalytic activity in the sorbitol hydrogenolysis, but a significant amount of $Ca(OH)_2$ has to be replenished in each run.

Although the results are very promising, it is necessary to know more about what is happening to the catalyst as the number of cycles increases with the purpose of identifying the main causes of the deactivation. To achieve this goal, we characterized the solid catalyst used in the reaction. First, and with the aim of obtaining more information about the used NiRuCa-HT catalyst after the first run, XRD characterization was conducted on the dried solid (see Fig. S3 in Supplementary material). $CaCO_3$ diffraction peaks (JCPDS 00-001-0837) were observed, and no peaks corresponding to Ru° and/or Ni° were detected, which indicated that these two species are highly dispersed in the used catalyst. The role of calcium carbonate in the deactivation should be negligible. Fig. 4 shows that in the second run, where this carbonate has already formed, the glycols yield is similar to that of the first run, in which calcium carbonate was not present.

Moreover, the X-ray photoelectron spectra of the Ru 3d and Ni 2p regions of fresh and used (one and five runs) NiRuCa-HT are shown in Fig. 5. The aim is to follow the evolution of the oxidation state of the ruthenium and nickel species with the number of runs. In this case, the Ca in $CaCO_3$ (347.6 eV) was used as the reference signal [24] (as shown in Fig. S3). The Ru 3d region is shown in Fig. 5A. For the sake of clarity, only the deconvolution for Ru $3d_{5/2}$ components is shown. The two components correspond to ruthenium in the reduced state and to the presence of RuO_x species in the used catalyst, the latter at 282.1 eV [22]. The fresh NiRuCa-HT spectrum is the same as that shown in Fig. 3, but not all deconvolutions are included. As we have already mentioned, the peak at 289.0 eV corresponds to the CO_3^{2-} of the $CaCO_3$ present in the catalyst. Concerning the Ni 2p region of the used catalyst (Fig. 5B), the component at ca. 855.0 eV is due to NiO species [29], while the peak at 852.3 eV suggests the presence of Ni° species. Its intensity increases with the number of runs. This result could indicate a minor interaction between the metals (Ni and Ru), which could partially explain the observed deactivation. Finally, Fig. 5B shows a third component for nickel at 857.5 eV on the used catalyst. The intensity of this signal does not change significantly with the number of runs. This component could be associated with the nickel hydroxide species present on the surface of the used catalyst.

In Table 3, the binding energies of the Ru 3d and Ni 2p levels and the surface atomic ratios Ru/Ca, Ni/Ca and Ni/Ru are recorded for the used NiRuCa-HT catalyst after one and five runs. Among the total ruthenium exposed, more than half appears as metallic ruthenium. No clear trend can be identified with the number of runs, but it

seems that the amount of metallic Ru is lower when the catalyst is used. The exposed nickel appears almost entirely as Ni^{2+} in the fresh sample, and the amount of metallic nickel species (Ni°) on the surface of the catalyst clearly increases with the number of cycles. Concerning the Ru/Ca and Ni/Ca ratios, a significant increase is observed when the catalyst is used for 5 runs, which is in agreement with the dissolution and consequent loss of $Ca(OH)_2$ during the reaction. As a result, the Ni/Ca and Ru/Ca ratio is larger for the used catalysts. Ni/Ru is likewise higher for the used catalysts than for the fresh catalyst.

The catalyst is not stable in the reaction medium due to the solubilization of the basic $Ca(OH)_2$ support during the reaction as a consequence of the formation of acidic by-products. However, when reutilization experiments were conducted by incorporating fresh $Ca(OH)_2$ to replenish the solubilized support, the yield of glycols is stable for three runs and decreases moderately in the fourth and fifth runs. This behavior is noteworthy because the few experiments reported in the literature on reusability show significantly faster deactivations or catalysts that are stable but with very high ratios of loaded catalyst to initial sorbitol, which are therefore not comparable with our results.

4. Conclusions

The results indicate that when ruthenium is supported directly on an alkaline promoter, such as $Ca(OH)_2$, a significant increase in the yield of glycols was observed with respect to that observed for alumina supported Ru catalyst, even when the basic oxide was added separately to the medium reaction. It suggests that it is important to have intimate contact between the ruthenium species and the basic promoter.

A promoting effect of Ni on the RuCa-HT catalyst was also clearly observed, reaching a 46% glycol yield after 4 h of reaction, which could be explained by the interaction between Ni and Ru (electronic transfer from Ni to Ru, data from TPR and XPS techniques).

The NiRuCa-HT catalyst, that with the best catalytic properties, was not stable in the reaction medium because of the high solubility of the basic $Ca(OH)_2$ support under the reaction conditions. However, adding an sacrificial amount of $Ca(OH)_2$ equivalent to the amount of support that was solubilized during each run resulted in a slowing down of the deactivation rate.

Acknowledgments

Financial support from the Spanish Ministry of Economy and Competitiveness (CTQ2012-38204-C03-01) is gratefully acknowledged. I.M.L. thanks CSIC (JAE-Predoctoral grant) for her financial support.

Appendix A. Supplementary data

Supplementary data associated with this article can be found, in the online version, at http://dx.doi.org/10.1016/j.apcatb.2015.12.005.

References

[1] D. Reyes-Luyanda, J. Flores-Cruz, P.J. Morales-Pérez, L.G. Encarnación-Gómez, F. Shi, P.M. Voyles, N. Cardona-Martínez, Top. Catal. 55 (2012) 148–161.
[2] P.L. Dhepe, A. Fukuoka, Catal. Surv. Asia 11 (2007) 186–191.
[3] P. Yang, H. Kobayashi, A. Fukuoka, Chin. J. Catal. 32 (2011) 716–722.
[4] A. Fukuoka, P.L. Dhepe, Angew. Chem. Int. Ed. 45 (2006) 5161–5163.
[5] A. Wang, T. Zhang, Acc. Chem. Res. 46 (2013) 1377–1386.
[6] J.J. Bozell, G.R. Petersen, Green Chem. 12 (2010) 539–554.
[7] J. Sun, H. Liu, Green Chem. 13 (2011) 135–142.
[8] M. Banu, P. Venuvanalingam, R. Shanmugam, B. Viswanathan, S. Sivasanker, Top. Catal. 55 (2012) 897–907.
[9] N. Li, G.W. Huber, J. Catal. 270 (2010) 48–59.
[10] L. Ye, X. Duan, H. Lin, Y. Yuan, Catal. Today 183 (2012) 65–71.
[11] L. Zhao, J.H. Zhou, Z.J. Sui, X.G. Zhou, Chem. Eng. Sci. 65 (2010) 30–35.
[12] K.L. Deutsch, D.G. Lahr, B.H. Shanks, Green Chem. 14 (2012) 1635–1642.
[13] T. Soták, T. Schmidt, M. Hronec, Appl. Catal. A 459 (2013) 26–33.
[14] X. Chen, X. Wang, S. Yao, X. Mu, Catal. Commun. 39 (2013) 86–89.
[15] I.M. Leo, M.L. Granados, J.L.G. Fierro, R. Mariscal, Chin. J. Catal. 35 (2014) 614–621.
[16] M. Banu, S. Sivasanker, T.M. Sankaranarayanan, P. Venuvanalingam, Catal. Commun. 12 (2011) 673–677.
[17] J. Sun, H. Liu, Catal. Today 234 (2014) 75–82.
[18] D.K. Sohounloue, C. Montassier, J. Barbier, React. Kinet. Catal. Lett. 22 (1983) 391–397.
[19] J.H. Zhou, M.G. Zhang, L. Zhao, P. Li, X.G. Zhou, W.K. Yuan, Catal. Today 147S (2009) S225–S229.
[20] F. Auneau, M. Berchu, G. Aubert, C. Pinel, M. Besson, D. Todaro, M. Bernardi, T. Ponsetti, R. Di Felice, Catal. Today 234 (2014) 100–106.
[21] C.D. Wagner, L.E. Davis, M.V. Zeller, J.A. Taylor, R.H. Raymond, L.H. Gale, Surf. Interface Anal. 3 (1981) 211–225.
[22] V. Mazzieri, F. Coloma-Pascual, A. Arcoya, P.C. L'Argentière, N.S. Fígoli, Appl. Surf. Sci. 210 (2003) 222–230.
[23] V. Choque, P.R. de la Piscina, D. Molyneux, N. Homs, Catal. Today 149 (2010) 248–253.
[24] M.L. Granados, M.D.Z. Poves, D.M. Alonso, R. Mariscal, F.C. Galisteo, R. Moreno-Tost, J. Santamaría, J.L.G. Fierro, Appl. Catal. B 73 (2007) 317–326.
[25] M.G. Cattania, F. Parmigiani, V. Ragaini, Surf. Sci. 211–212 (1989) 1097–1105.
[26] H.Y.H. Chan, C.G. Takoudis, M.J. Weaver, J. Catal. 172 (1997) 336–345.
[27] A.M. Hengne, N.S. Biradar, C.V. Rode, Catal. Lett. 142 (2012) 779–787.
[28] A. Masalska, Catal. Today 137 (2008) 439–445.
[29] H. Li, D. Yu, Y. Hu, P. Sun, J. Xia, H. Huang, Carbon 48 (2010) 4547–4555.